Marek Sadilek
František Fojtík
Zuzana Sadílková
Kamil Kolařík
Jana Petrů

A STUDY OF EFFECTS OF CHANGING THE POSITION OF THE TOOL AXIS AGAINST THE MACHINED SURFACE

Summary

The article focuses on monitoring the machined surface after it has been machined with different milling strategies. Different milling strategies refer to milling whilst changing the tool axis relative to the surface after finishing the free form milling.

The research focuses mainly on the geometric characteristics of the finished surface profile and residual stresses in the surface layer. The goal of the experimental work is to find an effective position of the tool axis, or an effective interval of the tool axis, in relation to the machined surface normal.

Practical applications of the results are focused on finishing milling of complicated shape surfaces especially in the production of moulds and dies for the automotive and aerospace industries. The technology is based on the substitution of three-axis milling for multi-axis milling, i.e. mainly 5-axis simultaneous milling.

*Key words:*   *tool axis, milling, residual stress, surface roughness, CAM system*

1. Introduction

Current CAD/CAM systems offer a host of automatic features and especially improvements that contribute to increasing efficiency in machining. The most progressive improvements refer to moulds, dies, cutting tools, parts for the aerospace industry, cylinder heads, turbine blades and paddle wheels and other complicated shape parts needed in various sectors of engineering industry. Developers of source codes CAMs systems attempt to simplify and facilitate the work of programmers of CNC machine tools by creating user-friendly software which is operated intuitively. One of the main interests is to optimise the toolpath. However, no CAM system can resolve the issue of optimising the tool axis angle to achieve the required quality of a machined surface.

2. Standard milling – without changing tool axis position

During standard milling with ball end milling cutters, when the material and the tool axis inclination equal 90 degrees (Fig. 1), a spherical cutting edge has zero cutting speed at the tool axis. The tool merely pushes the milled material at that place. Because of that, undesirable effects, such as chip contraction, increase in the cutting temperature, increase in

vibrations, and increased creation of a build-up edge can appear [20], [22]. These phenomena result in reduced quality of the milled surface and decreased tool durability [31]. Fig. 1 shows possibilities of tool inclination toward the surface normal.
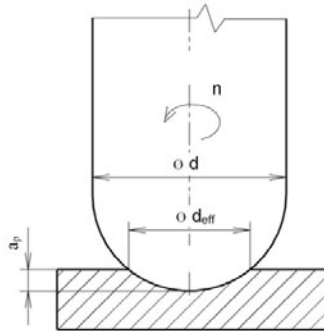
Fig. 1 Milling strategy without tool axis inclination angle (with the effective diameter of the cutter)

During the milling strategy in which the position of the tool axis is $\beta_{n(f)} = 0°$ there is a substantially reduced effective cutter diameter d_{eff}. This happens especially at small depths of cut a_p. For this reason, there is a substantial reduction in effective cutting speed v_{ceff}.

The effective diameter of the cutting tool during milling without tool inclination is calculated according to the following relationship:

$$d_{eff} = 2 \cdot \sqrt{a_p \left(d - a_p \right)}$$

(1)

where: d_{eff}, mm   - effective tool diameter

   a_p, mm   - axial depth of cut,

   d, mm   - tool diameter.

3. Milling strategy with tool axis inclination angle

The phenomena mentioned in the previous chapter can be eliminated by changing the tool axis position in relation to the milled piece, i.e., by inclination of the tool or the piece. Fig. 2 shows possibilities of tool inclination toward the surface normal.
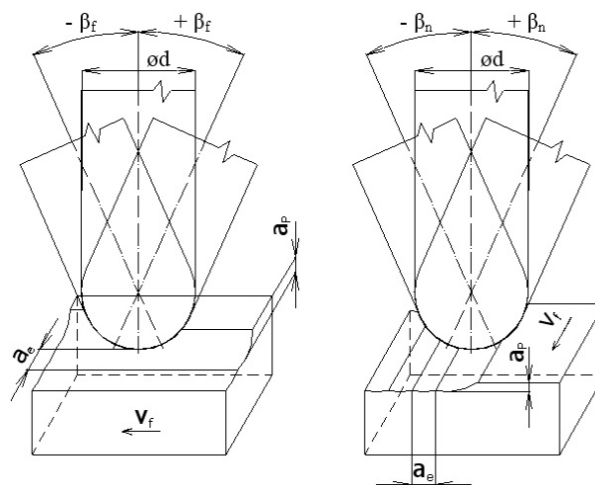
(a) Tilt in feed direction   b) Tilt in pick feed direction

Fig. 2 Milling strategy with tool axis inclination angle [18]

A feed direction is very important. If the feed direction is the so called "pulled direction" (Fig. 3a), the tool action is more silent and the surface of the milled material is

smoother as opposed to the so called pushed feed direction (Fig. 3b). These two ways can be used for the inclination in the feed direction as well as for the inclination that is perpendicular to the feed direction [18].
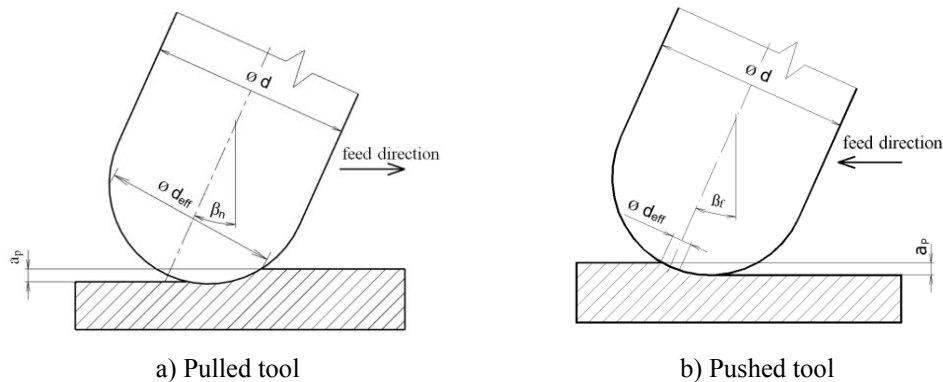

a) Pulled tool   b) Pushed tool

Fig. 3 Tool axis inclination angle in feed direction

Tilting the tool changes the effective cutter diameter, thus changing the effective cutting speed. The effective diameter of the pulled milling cutter is calculated according to the following relationship [21]:

$$d_{\text{eff}} = d \cdot \sin\left[\arccos\left(\frac{d - 2\,a_{\text{p}}}{d}\right) + \beta_{\text{f}}\right] \tag{2}$$

where: d_{eff}, mm   - effective tool diameter,

a_{p}, mm   - axial depth of the cut,

β_{f}, °   - tool axis inclination angle in the feed direction,

d, mm   - tool diameter.

In equation (2) the "+" sign is replaced at β_{f} with a "-" sign when the milling tool is pushed. According to this mathematical expression pulling makes a better use of the tool. Specific courses according to the specified cutting conditions (presented in the experimental section) are shown in Fig.4.
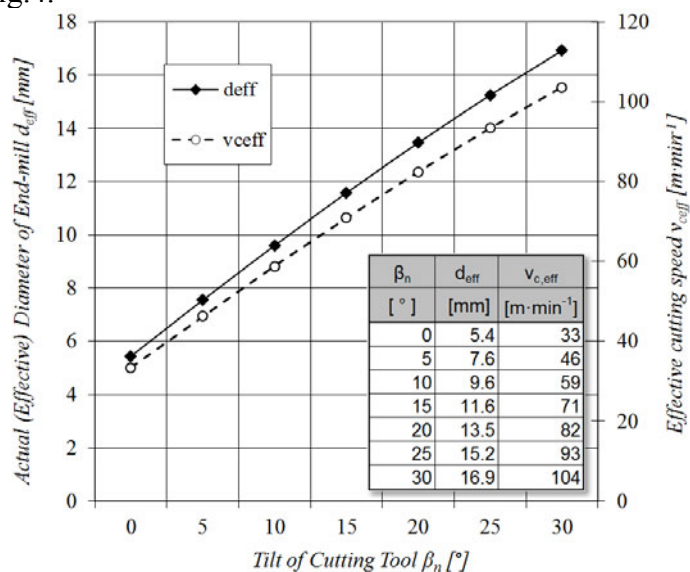

β_{n}	d_{eff}	$v_{c,\text{eff}}$
[°]	[mm]	[m·min^{-1}]
0	5.4	33
5	7.6	46
10	9.6	59
15	11.6	71
20	13.5	82
25	15.2	93
30	16.9	104

Fig. 4 The relationship of the effective tool diameter d_{eff} and the effective cutting speed $v_{c\text{eff}}$ at the angle of tool inclination β_{n}, ($d = 25$ mm, $a_{\text{p}} = 0.3$ mm, $v_{\text{c}} = 153$ m·min^{-1}, $n = 1950$ min^{-1})

Scientific literature describes the use of the tool axis inclination angle relative to the normal of the machined surface in the range of 10 to 30°. Scientific contributions often give the location of the tool axis at 15°. References [1],[2] indicate the range of 10 to 20°.

When milling complicated shaped surfaces there is a need to use different milling strategies. To maintain a constant tool axis inclination angle (or interval) to the normal surface workpiece it is necessary to use multi-axis milling. In these complicated, but far more frequent cases, the index 3-axis machining cannot be used. It is necessary to use the 5-axis simultaneous milling.

4. Experimental work

The experimental part describes the investigation aimed at monitoring the machined surface after machining different positions of the tool axis relative to the surface normal.

The machinability of steels using a CNC machine has been studied by many researchers [3], [4], [32], but these publications do not deal with problems related to the geometric characteristics of the finished surface profile and residual stresses in the surface layer.

Studies of machined surface topography during changing orientations of the tool axis can be found in literature [1], [6], [7], [8], [9]. Studies of the contact of the tool with the workpiece are described in [1], [10], [11]. Studies of optimising the cutting conditions and their influence on cutting forces are described in [1], [6], [1], [12], [10], [13]. Deformation deflection of the cutting tool or machined parts is defined in [1], [14]. The issue of durability of the cutting tool is discussed in [16]. Shape and chip geometry are given in [1], [6].

Seven positions (tilts) of the tool in a direction perpendicular to the tool feed were analysed. Each sample has a size of 20 x 20 mm. The present experimental research focuses only on the subset of extensive experiments identified by the authors. In the experiments a milling machine FSS 80 CNC (indexing 4-axis milling canter, CNC control system MEFI 856) was used. Changing the orientation of the axis was perpendicular to the feed by $\beta_n = 0$ ° to $\beta_n = 30°$ partitioned in 5°.

The machining strategy was "zig zag", a combination of climb and conventional milling. Method of tool feed was pulled tool. A cutting fluid was used. The workpiece material was 1.4313 (422960, X3CrNiMo13-4 + QT900). This is chromium nickel martensitic stainless steel with molybdenum addition. The machinability of these steels is adversely affected by their strong tendency towards cold hardening, low thermal conductivity and good toughness properties.

Table 1 Cutting conditions and theoretical surface roughness

Cut depth	Endmill diameter	Spindle rev.	Cutting speed	Theoretical surface roughness				Cut width	Feed per tooth
				Pick feed direction		Feed direction			
				Rz	Ra	Rz	Ra		
a_p	d	n	v_c					a_e	f_z
mm	mm	min^{-1}	m·min^{-1}	μm		μm		mm	mm
0.3	25	1 950	153	3.12	0.80	3.12	0.80	0.558	0.558

The cutting tool was a ball end milling cutter (Fig. 5) with cutting inserts (2 flutes, coating 8040 [17]), cutting geometry of the cutting insert: $\gamma_p = 0°$ a $\gamma_f = $ -7° to 14° [17], cantilever length (overhang) $l_n = 110$ mm. The cutting conditions are presented in Table I.

Fig. 5 Tool holder with cylindrical shank - type K2-SRC and insert type RC (tools by Pramet company) [17]

The measurement of the surface roughness parameters was performed on a portable touch profilometer SurfTest SJ-401 by Mitutoyo. The measurement of the machined surface was carried out in accordance with the standard DIN EN ISO 4288. The parameters Rz and Ra (the maximum height of the profile and the arithmetical mean deviation of the assessed profile) were measured 10 times in the feed direction and pick feed direction. The standard uncertainty type A (U_A), the standard uncertainty type B (U_B), the combined standard uncertainty U_C and the expanded uncertainty U were set. The actual value was a 95% probability within the boundaries of the value of the expanded uncertainty.

Table 2 shows roughness of the machined surface (for the cases of 7 tool axis inclination angles) and deviations from the theoretically calculated surface roughness in the feed direction and the pick feed direction (theoretical surface roughness $Rz = 3.12$ µm and theoretical surface roughness $Ra = 0.8$ µm).

Fig. 6 shows advantages of the tilting tools for achieving an improved machined surface. During the tilt of the tool to $\beta_n = 5°$ and 10° there is a significantly improved parameter Rz. (from $Rz = 8.9$ and $Rz = 10.4$ µm to the values near 4 µm measured in both directions). When the inclination is larger ($\beta_n = 15°$ and $\beta_n = 20°$), a decrease in the roughness in the feed direction and increased roughness in the pick feed direction are noticed. Upon a further increase in the tool tilting an increase in roughness in both directions was measured.

Table 2 The measured surface roughness and deviations from the theoretical roughness

Tool axis inclin. angle	Pick feed direction			Feed direction			Pick feed direction			Feed direction		
β_n	Rz		Dev.	Rz		Dev.	Ra		Dev.	Ra		Dev.
°	µm		%	µm		%	µm		%	µm		%
0	8.90	± 0.76	185	10.40	± 2.42	233	1.65	± 0.21	106	2.22	± 0.63	178
5	4.23	± 0.40	36	3.69	± 0.62	18	0.75	± 0.06	-6	0.79	± 0.12	-2
10	4.17	± 0.45	34	3.74	± 0.79	20	0.67	± 0.08	-16	0.64	± 0.09	-20
15	4.60	± 0.46	48	3.29	± 0.63	6	0.78	± 0.09	-2	0.55	± 0.09	-31
20	5.26	± 0.46	69	3.07	± 0.90	-2	0.92	± 0.07	15	0.56	± 0.14	-31
25	5.20	± 0.43	67	3.57	± 1.21	14	0.89	± 0.09	11	0.66	± 0.15	-18
30	5.57	± 0.72	79	4.04	± 0.98	29	0.96	± 0.16	20	0.94	± 0.44	18

Similar courses (similarity bathtub curve) are recorded in other studies conducted by other authors under different machining conditions (machining, cutting tools, machine tools, cutting conditions, etc).

The use of a suitable tilt of the tool can result in an improvement in the surface roughness parameter Rz at approximately 200% (the parameter Ra is improved by approximately 180%).

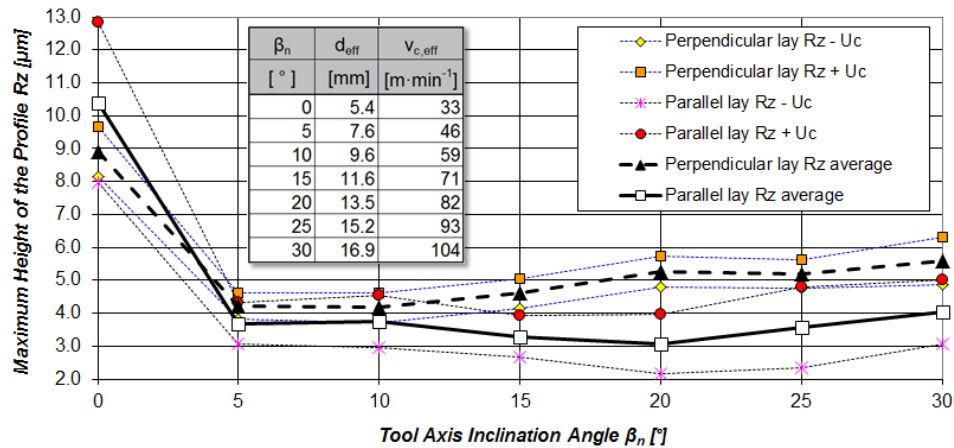**Fig. 6** Surface roughness (Rz) dependence on tool axis inclination angles (mat. 1.4313, $d = 25$ mm, $a_p = 0.3$ mm, $v_c = 153$ m·min^{-1}, $f_z = a_e = 0.558$ mm)

During machining it is necessary to select the appropriate cutting tool geometry for the machining method. Fig. 7 shows the insert with the disadvantage cut out of the so-called transition edge. By changing the position of the tool axis the real cutting geometry of the cutting tool is changed. However, in this case, there is no significant change in the geometry of the insert, see Fig. 7. Here, there is no cutting out of the transition edge. Therefore, there is no increase in surface roughness at a higher tilt due to large changes in the real cutting geometry.

The limiting angle of this insert is $\beta_{n,f} = 27.2°$. If the tilt is above this angle, the tool cut will provide unsuitable tool geometry, see. Fig. 7. This finding corresponds with the analytical calculations of the machined surface creations whilst changing the position of the tool axis as given in literature [30].
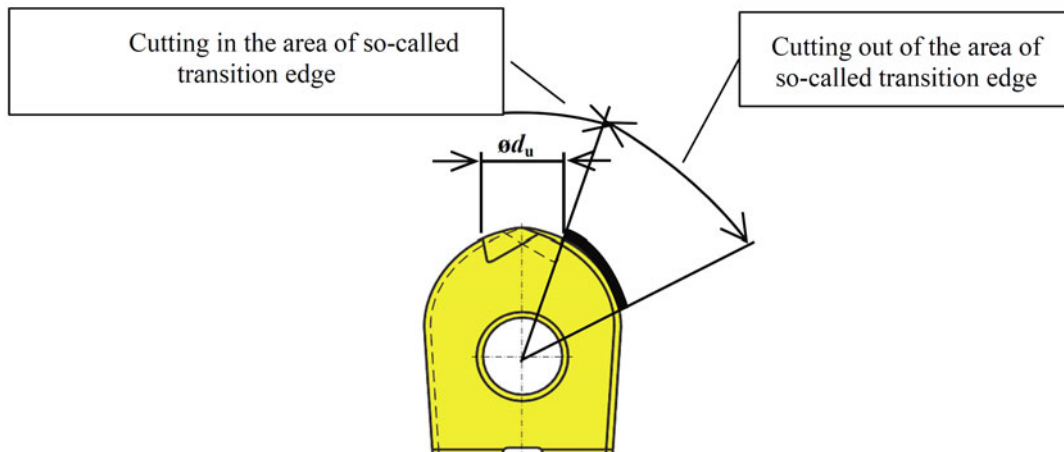

Fig. 7 Transition edge of insert with marked disadvantage of cutting in the area of so-called transition edge ($ød_u$ – diameter of transition edge)

Deviations of the theoretically calculated roughness ($Rz = 3.12$ µm and $Ra = 0.8$ µm) from the actually measured value are presented in Fig. 8. These deviations were measured in two directions of the tool feed. Fig. 8 shows smaller deviations in the inclined tool than in the not inclined tool when $\beta_n = 0°$. It is interesting that negative deviations of parameter Ra in the tool feed direction were achieved. They were reached when the surface roughness was smoother than the theoretically calculated roughness (smoother than is theoretically possible). This fact confirms the opinion of experts to prioritise the parameter Rz against Ra, when for practical verification of surface roughness the Rz parameter is fundamental. Furthermore, it confirms the necessity of measuring 3D surface parameters instead of 2D parameters [19], [27], [23].

For practical application, the calculation of the maximum height of the profile *R*z, which can be found in the CSN EN ISO 4287 and CSN EN ISO 4288 standards, is sufficient:

$$Rz = R \cdot \left(1 - \sqrt{1 - \frac{a_e}{4 \cdot R^2}} \right) \tag{3}$$

Where: *R*z, mm   - maximum height of the profile,
        R, mm   - cutter radius,
        *a*e, mm   - depth of the cut.
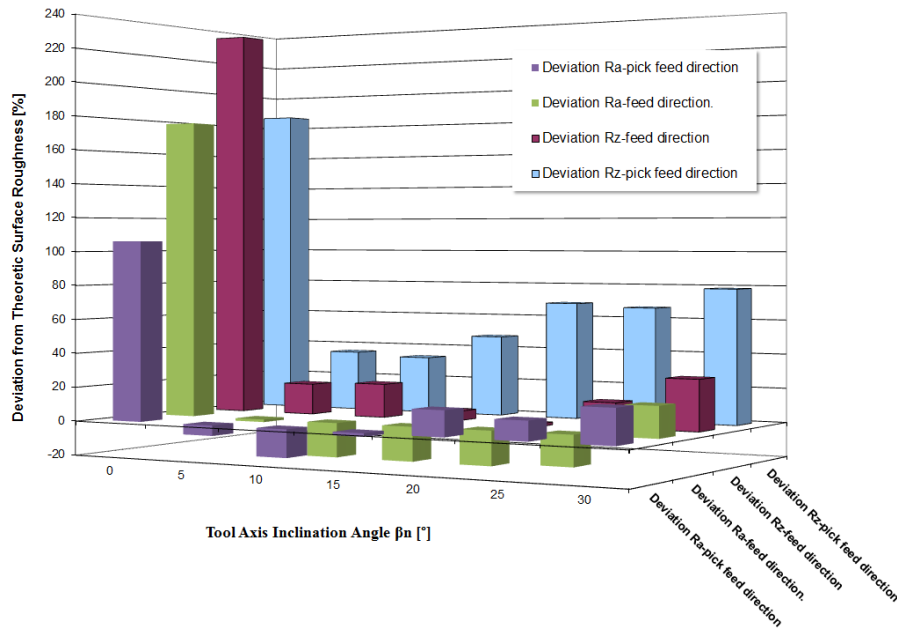
Fig. 8 Deviations of the measured surface roughness parameters from the theoretically computed
*R*z = 3.12 μm and *R*a = 0.8 μm (*d* = 25 mm, *a*e = *f*z = 0.558 mm)

4.1 Use of X-ray diffraction technique for the measurement of residual stress

In the surface layer of the workpiece residual stresses are introduced due to the technology of machining. Residual stresses remain there and still operate without any external load even upon completion of the manufacturing process [20], [19], [23], [27]. There is a presumption that the influence of changing the position of the tool axis will affect the surface layer of the workpiece.

In recent years, a number of experimental methods for measuring residual stresses have been developed. Classification methods for detecting residual stress, e.g. mechanical, diffraction, magnetic, ultrasonic and indirect methods, can be applied to many aspects, such as the residual stress measuring. These methods can be dependent on the extent to which the integrity of the examined elements, i.e. non-destructive, destructive and semidestructive elements, is affected. A review of methods for the determination of residual stresses and their distribution according to different criteria can be found in literature [25], [26], [28].

The essence of X-ray tensiometry is using X-rays diffraction on crystals to measure changes in the atomic lattice spacing of planes caused by tensile stress.

The residual stress measurements were performed with a vertical θ - θ X'Pert PRO diffractometer in the ω-arrangement with CrKα radiation. The diffraction profile {211} of the α-Fe phase was measured. The dependences of $2\theta_{211}$ versus $\sin^2\psi$ were measured in three azimuths, σ_0, σ_{45} and σ_{90}. The X-ray elastic constants ½ s_2 = 5.76·10^{-6} MPa^{-1}, − s_1 = 1.25·10^{-6} MPa^{-1} were calculated according to the Eschelby – Kröner model [25]. The presented residual

stresses are mean values of stress in the irradiated volume given by the irradiated surface area and the penetration depth which is approximately 5 µm for the used radiation. The indicated experimental errors of individual values are standard deviations from the algorithm of the residual stress calculation by the "sin²ψ" method [25], [26].

Before measuring residual stresses by the "sin ² ψ "method diffraction patterns were made by applying the Debye - Scherrer method to the reflection back, see Fig. 9. The continuous character of the diffraction line {211} α-Fe indicates qualitatively the fine-grained isotropic polycrystalline material of the surface layers with a thickness of about 3-5 microns. This corresponds to an effective depth of the penetration of X-rays in the material. In this case, the application method "sin ² ψ" is absolutely correct.

Tool axis angle $\beta_n = 0°$ Tool axis angle $\beta_n = 5°$
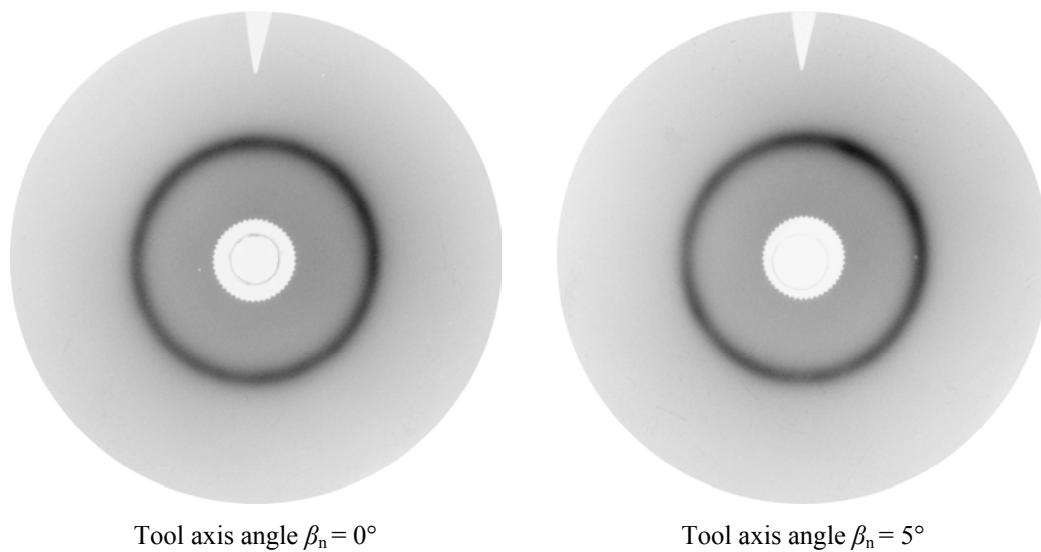
Fig. 9 Example of diffraction patterns by Debye - Scherrer method from areas of tool axis angle $\beta_n = 0°$ and 5°; $CrK\alpha$ radiation, cylindrical collimator with a diameter of 1 mm. Debye circle characterizes crystallographic planes {211}-Fe

The values of residual stresses were measured in three directions, i.e. in the tool feed direction (σ_0), in the pick feed direction (σ_{90}) and in the half the angle direction (σ_{45}), see Fig. 10.
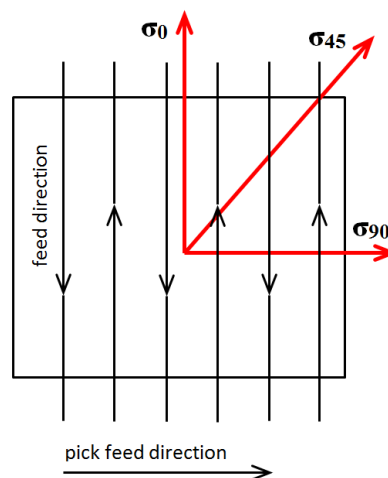
Fig. 10 Scheme of analysed surface with directions of residual stress measuring (tool feed direction (σ_0), pick feed direction (σ_{90}), half the angle direction (σ_{45}))

In the pick feed direction (direction σ_{90}), normal macroscopic tensile residual stresses were found, see Table 3. This is within the experimental error of zero value of the shear component.

In the direction identified as σ_{45}, normal macroscopic tensile residual stresses were also found, except for the tool axis position $\beta_n = 0°$, for which zero normal stress was found within the experimental error.

In the feed direction (direction σ_0), normal macroscopic pressure residual stresses were found for the tool axis inclination angles $\beta_n = 0°$ and $\beta_n = 5°$. Zero values of normal residual stresses were $\beta_n = 10°$. Tensile residual stresses were found from $\beta_n = 15°$ to 30°.

In the feed direction (direction σ_0), there were (within the experimental error) non-zero shear residual stresses in all the analysed tilts, see Table 4 and Fig. 12. This is probably caused by the rotation of the cutting tool.
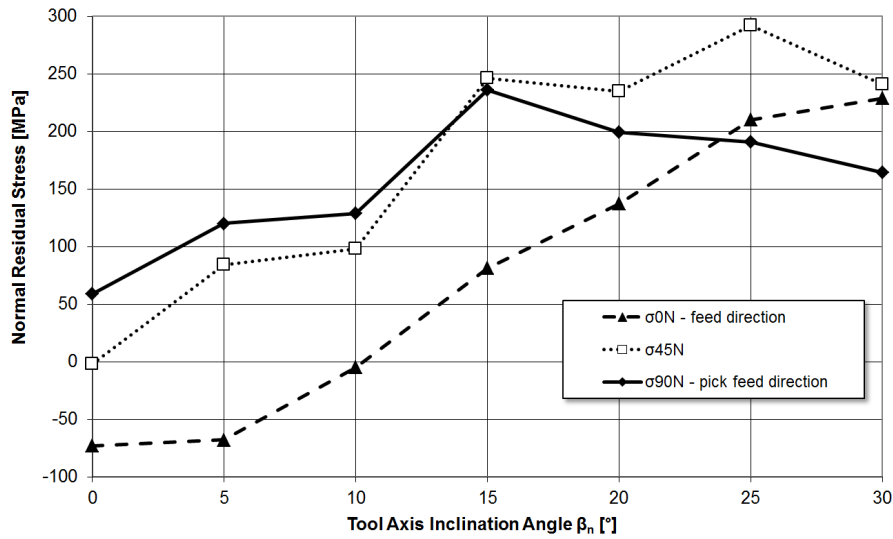
The maximum tilt of the cutting tool ($\beta_n = 30°$) caused the redistribution to the isotropic biaxial condition i.e. $\sigma_0 \approx \sigma_{90}$.

Table 3 Values of normal macroscopic residual stresses σ_0, σ_{45} and σ_{90} determined by XRD analysis at machined surfaces with positions of tool axis $\beta_n = 0°$ to 30°

Tool axis angle β_n	Normal residual stress					
	σ_0^N	$\Delta\sigma_0^N$	σ_{45}^N	$\Delta\sigma_{45}^N$	σ_{90}^N	$\Delta\sigma_{90}^N$
°	MPa					
0	-73	11	-2	14	59	15
5	-68	22	84	7	120	10
10	-5	17	98	10	129	12
15	81	19	246	4	236	14
20	137	16	235	10	199	12
25	210	11	292	9	191	12
30	229	14	241	13	164	11

Table 4 Values of shear macroscopic residual stresses σ_0, σ_{45} and σ_{90} determined by XRD analysis at machined surfaces with positions of tool axis $\beta_n = 0°$ to 30°
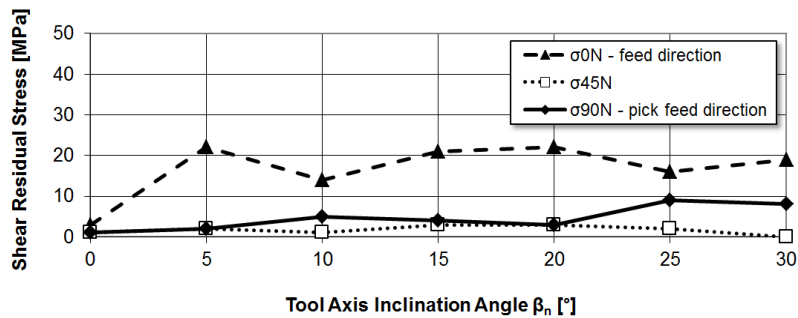
Tool axis angle β_n	Shear residual stress					
	σ_0^S	$\Delta\sigma_0^S$	σ_{45}^S	$\Delta\sigma_{45}^S$	σ_{90}^S	$\Delta\sigma_{90}^S$
°	MPa					
0	3	2	1	3	1	3
5	22	4	2	1	2	2
10	14	3	1	2	5	2
15	21	4	3	1	4	3
20	22	3	3	2	3	2
25	16	2	2	2	9	2
30	19	3	0	3	8	2

Fig. 11 Course of normal macroscopic residual stresses σ_0, σ_{45} and σ_{90} at machined surfaces
with positions of tool axis $\beta_n = 0\,°$ to $30\,°$

Fig. 12 Course of shear macroscopic residual stresses σ_0, σ_{45} and σ_{90} at machined surfaces
with positions of tool axis $\beta_n = 0\,°$ to $30\,°$

For each measured area, the quantity full width at half maximum (FWHM) was also determined as an average value of the FWHM of the diffraction doublet {211} α-Fe from measurements σ_0, σ_{45} and σ_{90} at $\psi = 0°$ and it represents the level of plastic deformation in the surface layers of the analysed samples. The experimental error of the determination is the standard deviation specified by the algorithm of the numerical treatment of diffraction profiles [26].

The values of the parameter W (average value of the FWHM of the diffraction doublet {211} α-Fe from measurements σ_0, σ_{45} and σ_{90} at $\psi = 0$ °) are shown in Table 5 and graphically presented in Fig. 13.

Table 5 Parameter W for tool axis inclination angle $\beta_n = 0\,°$ to $30\,°$

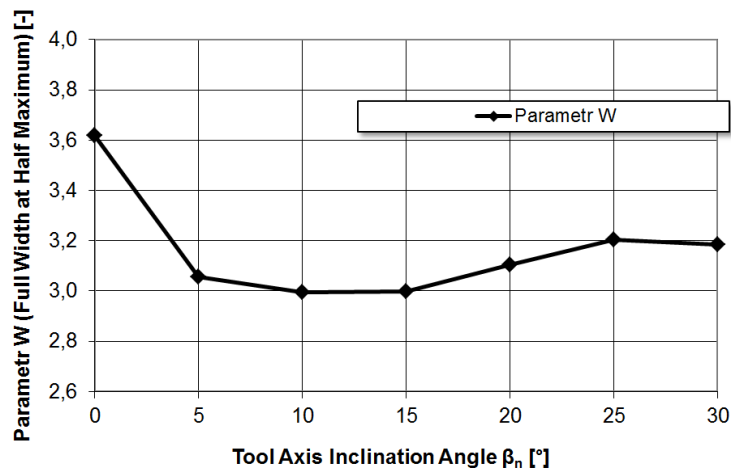| Tool axis angle	Parameter W (full width at half maximum)	
β_n	W	ΔW
°	-	-
0	3.619	0.049
5	3.055	0.022
10	2.994	0.025
15	2.998	0.034
20	3.104	0.030
25	3.205	0.020
30	3.185	0.042

Fig. 13 Course of W parameter for tool axis inclination angle $\beta_n = 0°$ to $30°$

The surface machined with $\beta_n = 0°$ has the highest values of the W parameter with the analysed diffraction doublet {211} α-Fe (see Table 5) in comparison with other machined surfaces. The parameter value W depends on the level of microscopic residual stress and the crystallite size in the surface layer and can be interpreted as a degree of plastic deformation. It means that the diffraction line width is proportional to the plastic deformation occurred during the cutting process.

Severe plastic deformation is also closely linked to the generation of dislocations. There exists a mutual relationship between dislocation density and the diffraction profiles´ shape, i.e. the higher the dislocation density, the larger is the diffraction line broadening. Quantitatively much higher broadening of the {211} α-Fe diffraction line for the zero tool axis angle is clearly seen in Fig. 13.

It is interesting to compare the course of the W parameter with the course of the surface roughness (maximum height of the profile Rz). There is an observed similarity in the course of the curves (similarity bathtub curve).

5. Conclusion

The investigation shows that the tool axis position has influence on the course of residual stresses in the surface layer. The machined surface during the standard position, i.e. the position in which the ball-end milling cutter is perpendicular to the machined surface (tool axis inclination angle $\beta_n = 0°$) is characterized by the lowest values of residual stresses in all three directions analysed. This finding is consistent with the theoretical assumption in which the stock removal occurs in the cutting zone with intensive plastic deformation. The elastic-plastic deformation also extends below the machined surface. The compression of the material discovered in the machined layer was caused by the milling in the area of the tool axis, where there is zero cutting speed. The compression of the material is due to the fact that part of the material cannot be cut to the set depth of cut because the cutting edge is not perfectly sharp. The results are the pressure residual stresses that are associated with an increase in the diffraction line. A specific case of such a case would be a small feed tool.

The above statement applies only when the cut temperature does not reach a certain level, when the surface layer is formed by tensile residual stresses. Other causes of the forming of tensile residual stresses are geometric aspects of the cutting tool, the effect of cutting conditions and finally the influence of the workpiece material.

The method of X-ray diffraction provides information about the state of the surface layer (without electrochemical removal of surface layers) to a maximum depth of 3-5 μm (with the use of a chromium X-ray tube). It distinguishes residual stresses of the first and the second type as opposed to the destructive methods. While mechanical destructive methods can be used regardless of the structural composition of the metal, an X-ray method is substantially limited to textured polycrystalline materials or materials with crystallites with dimensions larger than 10 μm, when the diffraction line breaks into discrete tracks [25],[26].

Future experiments (already in progress) will try to discover the course of residual stresses in greater thicknesses (up to 0.2 mm) using the hole drilling method. It is important to realise that the machined surface will remain residually stressed after the previous operations, before the main finishing milling operation starts. Residual stresses arise as superposition after all operations on the workpiece.

Experimental work leads directly to the finishing milling operation with changes in the tool axis inclination angle. It was expected that with increasing the tool axis inclination angle the tension would be a result of pressure residual stresses rather than of tensile residual stresses. The measurement using the X-ray diffraction method does not confirm this.

Follow-up experiments will study the dependence of micro hardness on the tool axis inclination angle. These experiments could discover greater dependence.

Surface roughness and residual stress affect the functional surfaces, durability and reliability of components, noise, run-time, friction, electrical resistance, heat transfer, fatigue strength, wear resistance, corrosion resistance, etc.

Free form finishing milling with a targeted change of the tool axis position can replace the grinding operation, i.e. the manual finishing grinding operation of free form surfaces. The reason is the improved quality of machined surfaces. The integrity of the ground surface is usually not satisfactory, e.g. in terms of thermal and tensile residual stresses affecting the surface layers. Therefore, research into these aspects of the machined surfaces is in high demand.

ACKNOWLEDGMENT

REFERENCES

[1]   Ko, T.J.; Kim H.S.; Lee S.S. Selection of the machining inclination angle in high-speed ball end milling, *International Journal of Advanced Manufacturing Technology* Vol. 17, 2001, pp. 163–170.

[2]   Schulz, H.; Hock, St. High-speed milling of dies and moulds-cutting conditions and technology, Annals of the CIRP 44 (1), 1995, pp. 35–38.

[3]   Krolczyk G, Gajek M, Legutko S. Predicting the tool life in the dry machining of duplex stainless steel, Eksploatacja i Niezawodnosc, *Maintenance and Reliability*, 2013, 15 (1), pp. 62–65.

[4]   Królczyk G., Legutko S., Stoić A. Influence of cutting parameters and conditions onto surface hardness of duplex stainless steel after turning process, *Tehnički Vjesnik - Technical Gazette*, No. 6, Vol. 20, 2013, pp. 1077-1080, ISSN: 1330-3651.

[5]   Bouzakis, K. D.; Aichouh, P.; Efstathiou, K. Determination of the chip geometry, cutting force and roughness in free form surfaces finishing, with ball end tools, *Int. J. Mach. Tools Manufact*. 43, 2003, p. 499– 514.

[6]   Ikua, B.W.; Tanaka, H.; Obata, F.; Sakamoto, S. Prediction of cutting forces and machining error in ball end milling of curved surfaces. I. Theoretical analysis, J. *Int. Soc. Prec. Eng. Nanotech.* 25, 2001, pp. 266–273.

[7]   Mizugaki, Y.; Hao, M.; Kikkawa, K. Geometric generating mechanism of machined surface by ball-nosed end milling, Annals of the CIRP 50 (1), 2001.

[8]   Mizugaki, Y.; Kikkawa, K. Teral, H.; Hao, M. Theoretical estimation of machined surface profile based on cutting edge movement and tool orientation in ball-nosed end milling, Annals of the CIRP 52 (1), 2003.

[9]   Toh, C.K. Surface topography analysis in high speed finish milling inclined hardened steel, *Precision Engineering.* 28, 2004, p. 386–398.

[10]   Kim, G.M.; Cho, P.J.; Chu, C.N. Cutting force prediction of sculptured surface ball-end milling using Z-map, Int. J. Mach. *Tools Manufact.* 40, 2000, p. 277–291.

[11]   Kim, G.M.; Kim, B.H.; Chu, C.N. Estimation of cutter deflection and form error in ball-end milling processes, *Int. J. Mach. Tools Manufact.* 43, 2003, p. 917–924.

[12]   Imani, B.M.; Sadeghi, M.H.; Elbestawi, M.A.. *An improved process simulation system for ball-end milling of sculptured surfaces,* Int. J. Mach. Tools Manufact. 38, 1998, 1089–1107.

[13]   Kim, G.M.; Chu, C.N. Mean cutting force prediction in ball-end milling using force map method, J. Mater. *Processing Technology.* 146 (3), 2004, p. 303–310.

[14]   Feng, H.-Y.; Menq, C.H. A flexible ball-end milling system model for cutting force and machining error prediction, J. *Manufacturing Science Engineering.* 118, 1996, p. 461–469.

[15]   Lee, C.M.; Kim, S.W.; Lee, Y.H., Lee, D.W. The optimal cutter orientation in ball end milling of cantilever-shaped thin plate, J. Mater. Process. Technol. 153/154, 2004, p. 900–906.

[16]   Kita, Y.; Furuike, H.; Kazino, Y.; Nakagawa, H.; Hirogaki, T. Basic study of ball end milling on hardened steel, *J. Mater. Process. Technol.* 111, 2001, p. 240–243.

[17]   Pramet Tools. D*ie & mould making tools*, Company catalogue, p. 44, 2004.

[18]   Sadílek, M.; Čep, R. Budak, I.; Sokovic, M. Aspects of Using Tool Axis Inclination Angle, *Strojniški vestnik - Journal of Mechanical Engineering*, 2011, vol. 57, no. 9, p. 681-688.

[19]   Adamczak, S., Miko, E., Čuš, F. A model of surface roughness constitution in the metal cutting process applying tools with defined stereometry. *Strojniški vestnik -Journal of Mechanical Engineering*, 2009, vol. 55, no. 1, p. 45-54.

[20]   Čep, R.; Janásek, A.; Martinický B.; Sadílek M. Cutting tool life tests of ceramic inserts for car engine sleeves. *Tehnički vjesnik/Technical Gazette*, No.2, Vol. 18, p. 203 – 209, 06/2011, ISSN: 1330-3651.

[21]   Peterka, J. Nový přístup výpočtu střední aritmetické odchylky drsnosti obrobeného povrchu při kopírovacím frézováním/A new approach of calculating the arithmetical mean deviation of roughness of the machined surface at the free form surface milling: Strojírenská technologie/*Manufacturing Technology, vol. IX, no.2,* 2004, *p. 28-32.*

[22]   Sadílek, M.; Čep, R.; Sadílková, Z.; Valíček, J.; Petřkovská, L. Increasing tool life in turning with variable depth of cut. *Materiali in tehnologije/Materials and technology*. 2013, vol.47, no.2, pp.199-203, ISSN:1580-2949.

[23]   Petřkovská, L.; Petrů J. *Engineering metrology and assembly*. VŠB-Technical university of Ostrava, 2012, p.106.

[24]   Biesinger, F.; Thiel, M.; Schulze, V.; Vöhringer, O.; Krempe, M.; and Wendt, U., , Characterization of surface and subsurface regions of HSC-milled steel", In: Schulz, H. (Editor), *Scientific Fundamentals of HSC*, Ed. Druckhaus, Munich, Germany, 2001, pp. 137-149.

[25]   Kraus, I.; Ganev, N. *Technické aplikace difrakční analýz/Technical applications diffraction analysis*. ČVUT, Praha 2004.

[26]   Kraus, I.; Ganev, N. *Difrakční analýza mechanických napětí/Diffraction analysis of mechanical stress*. 1 ed., Praha: ČVUT, 1995. p. 274, ISBN 80-01-01366-9.

[27]   Neslušan, M.; Turek, S.; Brychta, J.; Čep, R.; Tabaček M. *Experimentálne metódy v trieskovom obrábaní/Experimental methods in cutting operation* 1.ed. Žilina: EDIS, 2007. p. 343, ISBN 978-80-80-70-711-8. Chapter 3.2, s. 68-98.

[28]   Hauk, V. *Structural and Residual Stress Analysis by Nondestructive Methods*. Amsterdam: Elsevier, 1997. 654 s. ISBN-10: 0444824766.

[29]   Snyder, R. L.; Fiala, J.; Bunge, H. J. *Defect and Microstructure Analysis by Diffraction*. Oxford: Oxford Science Publications 1999. 808 s. ISBN-10: 0198501897.

[30]   Chen, J.S.; Huang, Y.K.; Chen, M.S. A study of the surface scallop generating mechanism in the ball-end milling process, *International Journal of Machine Tools & Manufacture,* 45, 2005, p. 1077–1084, 2005.

[31]   Ungureanu, N.S., Fiabilitatea si diagnoza/ Reliability and diagnosis, Editura Risoprint, Cluj Napoca, p.144, 2003, ISBN 973-656-554-8.

[32]   Čep, R.; Janásek, A.; Čepová, L.; Petrů, J.; Hlavatý, I., Car, Z.; Hatala, M. Experimental testing of exchangeable cutting inserts cutting ability/Eksperimentalno ispitivanje rezne sposobnosti izmjenjivih reznih umetaka, *Tehnicki Vjesnik,* 2013, *20*(1), 21-26.

Marek Sadilek
František Fojtík
Zuzana Sadílková
Kamil Kolařík
Jana Petrů
Department of Machining and Assembly,
Faculty of Mechanical Engineering, VŠB-
Technical University of Ostrava, 17.
listopadu 15/2172, 708 33 Ostrava, Czech
Republic
František Fojtík
Department of Mechanics of Materials,
Faculty of Mechanical Engineering, VŠB-
Technical University of Ostrava, 17.
listopadu 15/2172, 708 33 Ostrava, Czech
Republic
Kamil Kolařík
Department of Solid State Engineering
Faculty of Nuclear Sciences and Physical
Engineering, Czech Technical University
in Prague, Trojanova 13, Prague 2, Czech
Republic